Journal of Engineering Science and Technology
Vol. 10, No.11 (2015) 1422 - 1440

PHOTOVOLTAIC BASED SHUNT ACTIVE FILTER FOR POWER QUALITY IMPROVEMENT USING ICOSΦ THEORY

VIJAYAKUMAR G.[1,*], ANITA R.[2]

[1]Department of EEE, K.S.R. College of Engineering, Tamil Nadu, India
[2]Department of EEE, Institute of Road and Transport Technology, Tamil Nadu, India
*Corresponding Author: vijayakumargovind@yahoo.com

Abstract

This paper presents an optimal operation of Photovoltaic based Shunt Active Filter as (PV-SAF) for significant energy conservation, harmonic mitigation and reactive power compensation. When the PV system generates excessive or equal power required to the load demand, then the coordinating logic disconnects the service grid from the load and with a consequent reduction of panel tariff and global warming gasses. The PV module is connected to the DC side of SAF through the DC-DC converter. Converter switch is controlled by fuzzy based Perturb & Observe (P&O) Maximum Power Point Tracking (MPPT) algorithm and it eliminates the drawback in the conventional PV system. The reference currents are extracted by the Fuzzy logic controller based ICosΦ control strategy. This proposed PV-SAF, if connected at the terminals of a small industry or a home or a small enlightening institution can avoid the use of interruptible power supply and individual stabilizer. An emulation using MATLAB Simulink is presented to validate the advantage of the proposed system.

Keywords: Shunt active filter, Perturb & Observe, Maximum power point tracking, DC-DC converter, Energy conservation.

1. Introduction

Recently, the percentage of the sensitive loads such as computers, medical equipment and devices in Information Technology has increased. These sensitive loads are operated continuously during a 24 hours period and require reliable power supply. If supplying unreliable power these devices bring severe losses to the domestic and industrial customers. Then again, increase the EMI problem; real and reactive power losses, which can cause harmonics phenomena on the line current. So the power qualities become more important to maintain the safety of

Nomenclatures

C_{SI}	Changes in output current
C_{SV}	Changes in output voltage
I_L	Load current
Is	Source current
MPPT	Maximum power point tracking
P&O	Perturb and observe
P_{PV}	Photovoltaic power
PV	Photovoltaic
SAF	Shunt active filter
Ta, Ty	Ambient temperature
THD	Total harmonic distortion
V_m	Peak instantaneous voltage
VSI	Voltage source inverter

electrical devices and customer satisfaction. The proposed PV-SAF is connected in shunt with the three-phase distribution system. The PV based SAF injects current of the same amplitude and reverse phase to that of the load current into the ac system, in order to compensate the source current.

The DC-link voltage is decreasing during the compensation. The SAF supported DC-link capacitor consumes more power from the distribution system for the continuous compensation. Taking these aspects into account, renewable power generation system integrated with SAF is proposed in this work. The PV-SAF is proposed for source current harmonic reduction, supply of real and reactive power to the load and satisfies the load demand. The interfacing inductor provides the isolation and filtering between the three-leg VSI and the distribution system.

At present, the nations have increased the use of PV system in the power system application. PV-SAF system has become favorable solutions for frequent power interruptions in a day [1]. ICosØ Control algorithm is attractive that the control scheme should be applicable in any practical power system under the operating conditions such as balanced source/load and unbalanced source/load. In the frequency domain, the device switching frequency of the SAF is kept generally more than twice the highest compensating harmonic frequency for effective compensation [2]. Correction in the time domain is based on the principle of holding the instantaneous values within some reasonable tolerances. An instantaneous error function is computed on-line, which is the difference between actual and reference current/voltage waveform. The greatest advantage of time domain correction is its fast response to changes in power system [3]. It is easy to implement and has very little computational burden.

The Mamdani type of fuzzy controller used for the control of SAF gives better results compared with the PI controller, but it has the drawback of a larger number of fuzzy sets and 49 rules. Though several control techniques and strategies had been developed there were still filter performance contradictions [4], these became primarily motivation for the current paper. This paper is focusing the performance of fuzzy logic controller based Icos ø algorithm, which is prominent one to analyze under transients. To validate current THD

observations, extensive simulations were performed and the detailed simulation results are included.

2. System Configuration

The power circuit of the proposed Photo-voltaic System based SAF topology namely PV-SAF is presented. The PV-SAF is designed to compensate the current disturbance at the load side. It is also designed to inject the real power generated by the PV system to load on whole day [5]. The PV-SAF consists of PV array, rectifier, converter, energy storage unit, VSI, filters and switches S_1, S_2, S_3, P_1, P_2, P_3 and R_1, R_2. The proposed circuit topology of the three phase PV-SAF is shown in Fig. 1. The proposed three phase PV-SAF operates in two modes as in Table 1: 1) compensation mode and 2) UPS Energy conservation mode. In the first mode, under normal condition the semiconductor S_1, S_2, S_3 switches are turned ON and R_1, R_2 turned OFF. When SAF detects difference in the current, then the SAF enter into compensation mode through the inductor. Three phase AC current is injected in shunt with desired magnitude, phase angle and wave shape for the compensation. In the second mode, when the PV system generates excessive or equal real power to the load demand, then the SAF enters into a UPS energy conservation mode. The system aims to transfer the power generated on the PV system to the AC load through the three-phase Voltage Source Inverter (VSI). The excessive power generation of the PV system turns ON the switch R_1 and turns OFF the switch R_2. During this mode, the switches S_1, S_2, S_3 are turned OFF and the switches P_1, P_2 and P_3 are turned ON as presented in Table 2.

Table 1. Control signals for semiconductor switches.

Mode	Control Signals					
	S_1	S_2	S_3	P_1	P_2	P_3
Compensation	1	1	1	1	1	1
UPS Energy Conservation	0	0	0	1	1	1

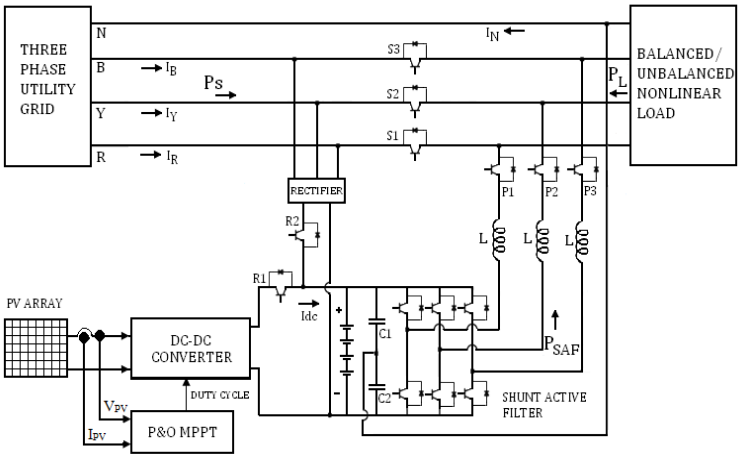

Fig. 1. Block diagram of the proposed PV-SAF.

Table 2. Battery control.

Condition	Control Signals		Battery Charging Unit
	R1	R2	
$\mathbf{P_{PV} \geq P_L}$	1	0	PV system
$\mathbf{P_{PV} < P_L}$	1	1	PV system & Rectifier

3. Detection of Disturbance

In I cos Ø algorithm, the grid source is required to supply only the real component of the load current. Remaining parts of load current i.e., reactive component and harmonics are to be compensated by the shunt active filter. The three phase instantaneous fundamental component of voltages can be represented [6] by Equation (1),

$$v_a = V_m \sin \omega t \, ; v_b = V_m \sin(\omega t - 120^0) \, ; v_c = V_m \sin(\omega t + 120^0) \quad (1)$$

where, a, b, c is phases a, b, c, respectively, V_m is peak value of the instantaneous voltage; the load current (I_L) contains fundamental and harmonic components. The fundamental component of the load current ($I_{Lfâ}$) is separated with the help of biquad low pass filter. Its output is fundamental component is delayed by 90^0 as represented by Equations (2), (3) and (4).

$$i_{Lfa} = I_{La,1} \sin(\omega t - \emptyset_{1a} - 90^0) \quad (2)$$

$$i_{Lfb} = I_{Lb,1} \sin(\omega t - \emptyset_{1b} - 120 - 90^0) \quad (3)$$

$$i_{Lfc} = I_{Lc,1} \sin(\omega t - \emptyset_{1c} + 120 - 90^0) \quad (4)$$

The real part of the fundamental component of load current is estimated as, at the time of negative zero crossing of the input voltage of phase a, i.e., ωt =180^0, instantaneous value of fundamental component of load current is $i_m \cos Ø$. The magnitude of the desired source current $|I_{s(ref)}|$ can be expressed as the magnitude of real component of fundamental load current in the respective phases, i.e., for phase a it can be written as $|I_{s(ref)}| = |\mathrm{Re}(I_{La})|$. To ensure balanced, sinusoidal currents to be drawn from the source, the magnitude of the desired source current can be expressed as the average of the magnitudes of the real components of the fundamental load currents in the three phases is gives as in Eq. (5).

$$|I_{s(ref)}| = \frac{|Re(I_{La})|+|Re(I_{Lb})|+|Re(I_{Lc})|}{3}; \; |I_{s(ref)}| = \frac{|I_{La}| \cos \emptyset_a + |I_{Lb}| \cos \emptyset_b + |I_{Lc}| \cos \emptyset_c}{3} \quad (5)$$

The voltage fluctuations in DC bus voltage of shunt active filter are also sensed and given to fuzzy controller, which calculates the current to be taken from the source to meet power loss in the inverter. This current is added to the average value of $|I_{s(ref)}|$. The three phase source voltages are used as templates to generate unit amplitude sine waves in phase with source voltages and they are expressed as Eq. (6),

$$U_a = 1 \sin \omega t \quad ; U_b = 1 \sin(\omega t - 120^0) \; ;; \; U_c = 1 \sin(\omega t + 120^0) \quad (6)$$

The desired (reference) source currents in the three phases are obtained by multiplying reference source currents with unit amplitude templates of the

phase to ground source voltages in the three phases as given in Eqs. (7), (8) and (9) respectively.

$$i_{sa(ref)} = \left|I_{s(ref)}\right| * U_a = \left|I_{s(ref)}\right| \sin \omega t \quad (7)$$

$$i_{sb(ref)} = \left|I_{s(ref)}\right| * U_b = \left|I_{s(ref)}\right| sin(\omega t - 120^0) \quad (8)$$

$$i_{sc(ref)} = \left|I_{s(ref)}\right| * U_c = \left|I_{s(ref)}\right| sin(\omega t + 120^0) \quad (9)$$

The equivalent block diagram of Icos ∅ algorithm is shown in Fig.2.

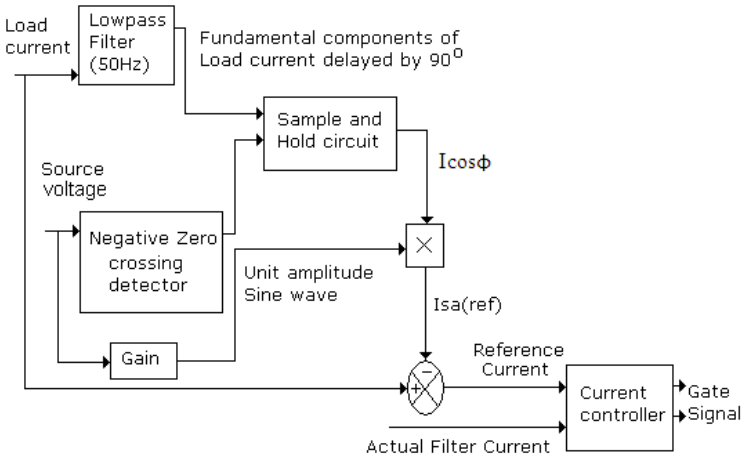

Fig. 2. Block diagram implementation of Icos ∅ algorithm for a phase.

The compensation currents to be injected by the shunt active filter are the difference between the actual load currents and the desired source currents represented in Eq. (10)

$$i_{a(comp)} = i_{La} - i_{sa(ref)};\ i_{b(comp)} = i_{Lb} - i_{sb(ref)};\ i_{c(comp)} = i_{Lc} - i_{sc(ref)} \quad (10)$$

During the transient condition the DC link capacitor voltage is varying, in order to obtain the power loss in the capacitor is calculated by fuzzy rule based method as shown in Fig. 3.

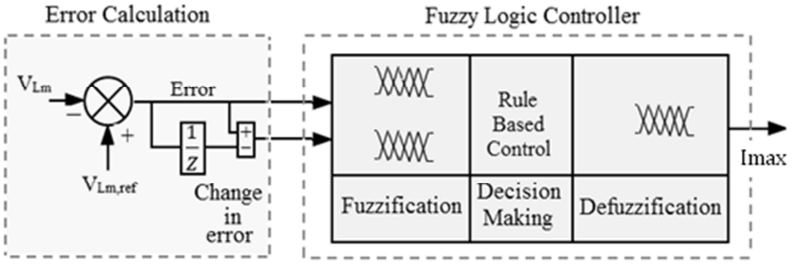

Fig. 3. Fuzzy based power loss calculation in inverter.

4. PV Array Modeling

PV arrays are built up with combined series/parallel combination of PV solar cells. The PV array requires DC-DC converter to regulate the output voltage under the sudden changes in weather conditions, which change the solar irradiation level as well as cell operating temperature. An equivalent circuit model of photovoltaic cell with DC-DC converter is shown in Fig. 4. The output voltage of the PV cell is a function of photo current that is mainly determined by load current depending on the solar irradiation level during the operation [7]. The PV cell output voltage is expressed as in Eq. (11).

$$V_o = \frac{AkT_c}{e} ln\left(\frac{I_p + I_o - I_c}{I_o}\right) - R_s I_c \tag{11}$$

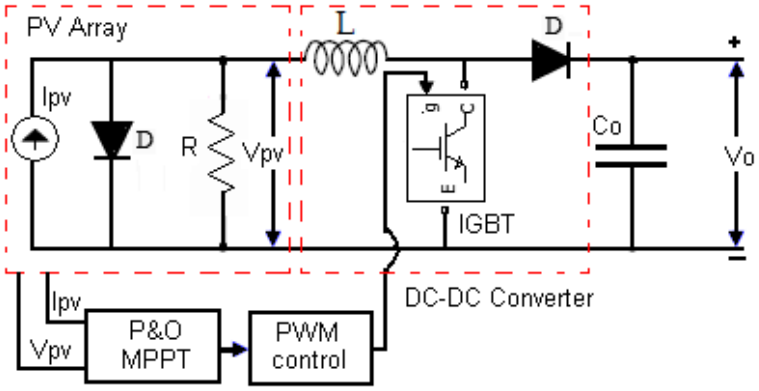

Fig. 4. PV Modeling boost converter with P&O MPPT algorithm.

where, e is the charge of electron, V_c is the output voltage of PV cell in volts, I_{ph} is the photo current in A, I_0 is the reverse saturation current of diode, k is Boltzmann constant, I_c is the cell output current in A, R is the cell internal resistance, T_c is the operating temperature of the reference cell 25 ^{0}c.

The design parameters I_{ph}, I_o, R_s and T_c are determined from the data sheet and I-V characteristics of the PV array [8]. The operating temperature of solar cell varies as a function of solar irradiation level and ambient temperature. The effect of change in ambient temperature and solar irradiation levels are represented in the model by the temperature coefficients $C_{TV\ and}$ C_{TI} are given in Eqs. (11) and (12). Where, β_T= 0.004 and γ_T= 0.06.Ta and T_y represent the ambient temperature of the cell and atmosphere.

$$C_V = 1 + \beta_T(T_a - T_x) \tag{12}$$

$$C_I = 1 + \frac{\gamma_T}{S_r}(T_x - T_a) \tag{13}$$

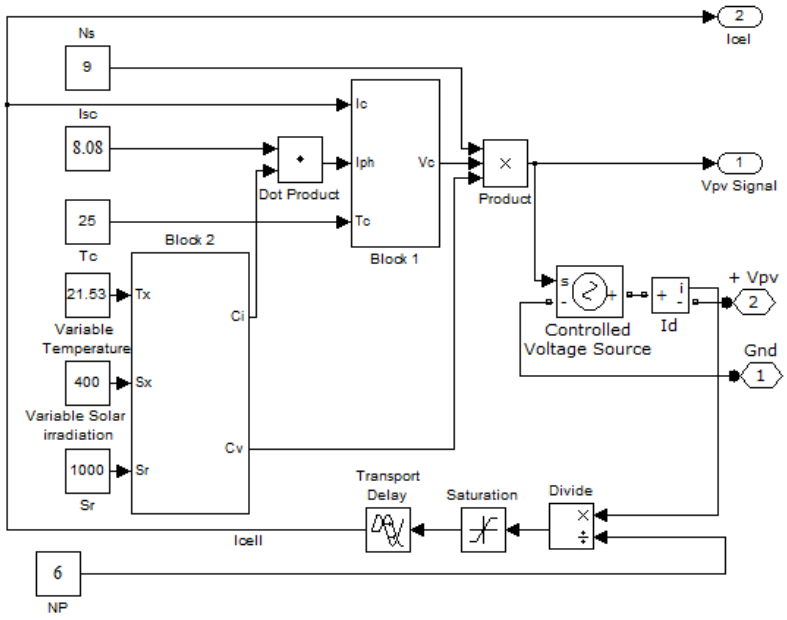

Fig. 5. Functional of photovoltaic array block diagram.

5. Control Method

5.1. PV MPP tracking control

Currently the most popular MPPT algorithm is Perturb and Observe (P&O) [9], where the current/voltage is repeatedly perturbed by a fixed amount in a given direction, and the direction is changed only if the algorithm detects a drop in power between steps. In the proposed work each perturbation of the controller gives a reference voltage, which is compared with the instantaneous PV module output voltage and the error is fed to a fuzzy controller, which in turns decides the duty cycle of the DC/DC converter. The process of perturbation is repeated periodically until the MPP is reached [10].

The computation of actual state (*k)* and previous state (*k*-1) of the parameters *V* and *I* are considered. The power is calculated from the product of actual and previous state V & I. According to the condition as represented in Fig. 6, the increment or decrement of reference voltage of the PWM pulse generator is obtained. The Simulink block diagram of the fuzzy controller based P&O MPPT is shown in Fig. 7. The inputs and output of fuzzy controller are expressed as a set of linguistics variables as shown in Fig. 7. Follows: NB-Negative Big, NS-Negative Small, Z-Zero, PS-Positive Small and PB-Positive Big. The output of the fuzzy is chosen form a set of semantic rules that lead to track the maximum power point of PV array. The set of rules chosen are shown in Fig. 8 and Table 3.

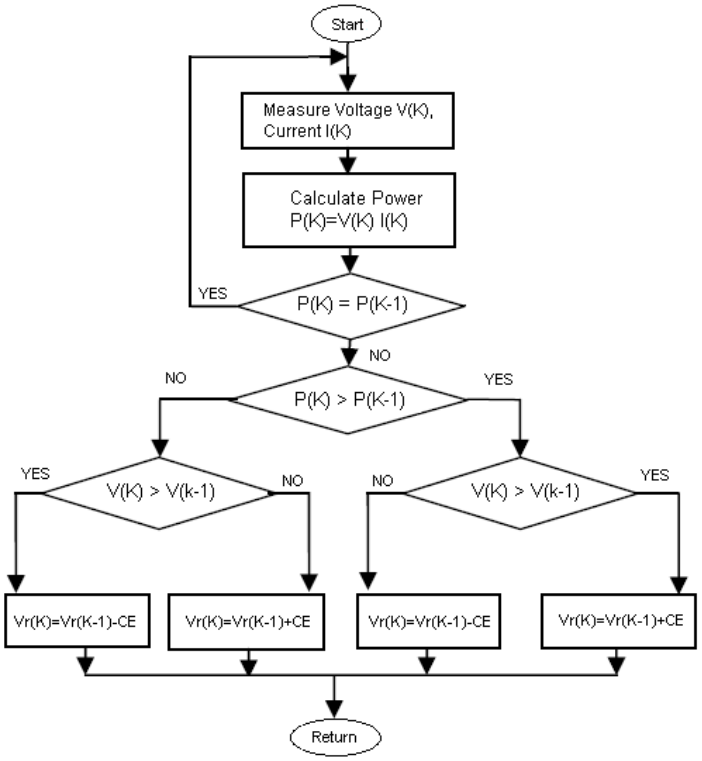

Fig. 6. Flow chart of P&O MPPT algorithm.

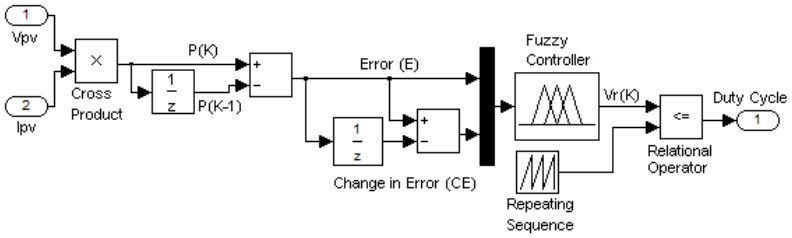

Fig. 7. Control structure of fuzzy P&O MPPT.

Table 3. Fuzzy rules for P&O MPPT method.

E/CE	NB	NS	ZE	PS	PB
NB	ZE	ZE	PB	PB	PB
NS	ZE	ZE	PS	PS	PS
ZE	PS	ZE	ZE	ZE	NS
PS	NS	NS	NS	ZE	ZE
PB	NB	NB	NB	ZE	ZE

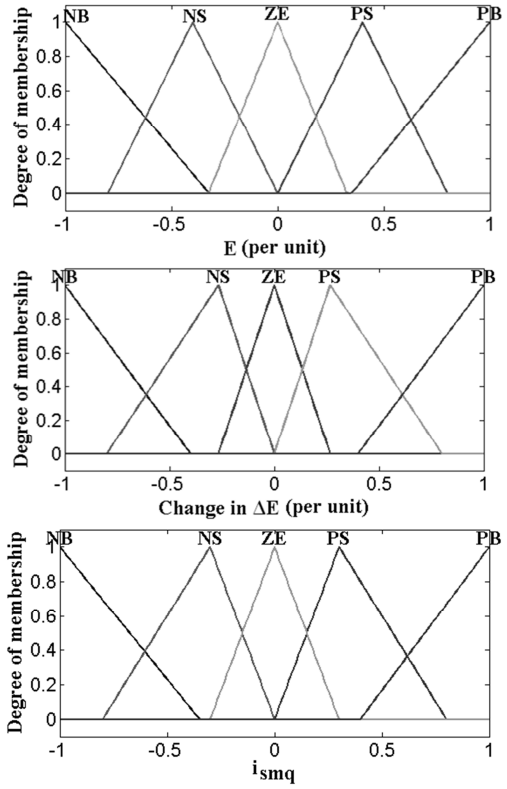

Fig. 8. Membership function for variable E, change in error CE and output.

5.2. SAF controller

The control system of SAF with fuzzy controller is shown in Fig. 9. This compensator solves harmonic problems in the source side. In the conventional controllers like P, PI and PID, the control parameters are fixed at the time of design. Hence, the conventional controllers offer good performance only for the linear system. When the operating point of the system is changed, the parameters of the conventional controllers should be designed again, and some trials and prior information of the systems are needed to design the parameters. The fuzzy controller overcomes the drawbacks of the conventional controllers [11-12]. The DC-bus voltage is first sensed and compared with DC reference voltage and error signal is generated. The error signal and its derivative are applied to fuzzy logic controller. Error signal is applied to Memory block and its output is subtracted from the error signal to obtain derivative of error signal.

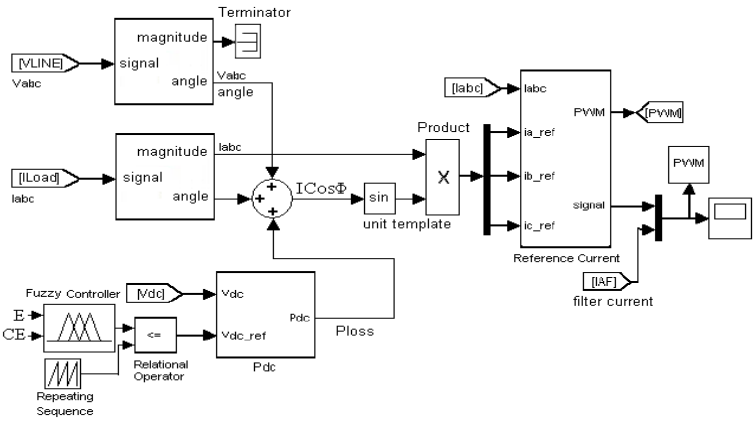

Fig. 9. Control of SAF.

The processed error signal is modulated using Sinusoidal Pulse Width Modulation (SPWM) to produce the required pulse to VSI for compensate the load voltage and current. To compare a sinusoidal frequency 50 Hz with a triangular carrier waveform $V_{carrier}$ with 20 kHz signal to produce the PWM pulses for three phase SAF. When the control signal is greater than the carrier signal, the switches are turned on, and their counter switches are turned off. The output voltage of the inverter mitigates harmonics. The two inputs and the output use seven triangular membership functions namely Negative Big (NB), Negative Medium (NM), Negative Small (NS), Zero (ZE), Positive Small (PS), Positive Medium (PM), Positive Big (PB). The type and number of membership functions (MFs) decides the computational efficiency of a FLC. The shape of fuzzy set affects how well a fuzzy system of If–then rules approximate a function. The membership values of input and output variables are shown in Fig. 10. Each input has seven linguistic variables; therefore there are 49 input label pairs. A rule table relating each one of 49 input label pairs to respective output label is given in Table 5 and the Eqs. (20) and (21).

$$E\ (error) = \left|V_{ref}\right| - |V_s| \tag{20}$$

$$\text{CE (Change in error)} = e(n) - e(n-1) \tag{21}$$

Table 4. Fuzzy rules for SAF voltage regulation.

E/CE	NB	NM	NS	ZE	PS	PM	PB
NB	PB	PB	PB	PM	PM	PS	ZE
NM	PB	PB	PM	PM	PS	ZE	NS
NS	PB	PM	PM	PS	ZE	NS	NM
ZE	PM	PM	PS	ZE	NS	NM	NM
PS	PM	PS	ZE	NS	NM	NM	NB
PM	PS	ZE	NS	NM	NM	NB	NB
PB	ZE	NS	NM	NM	NB	NB	NB

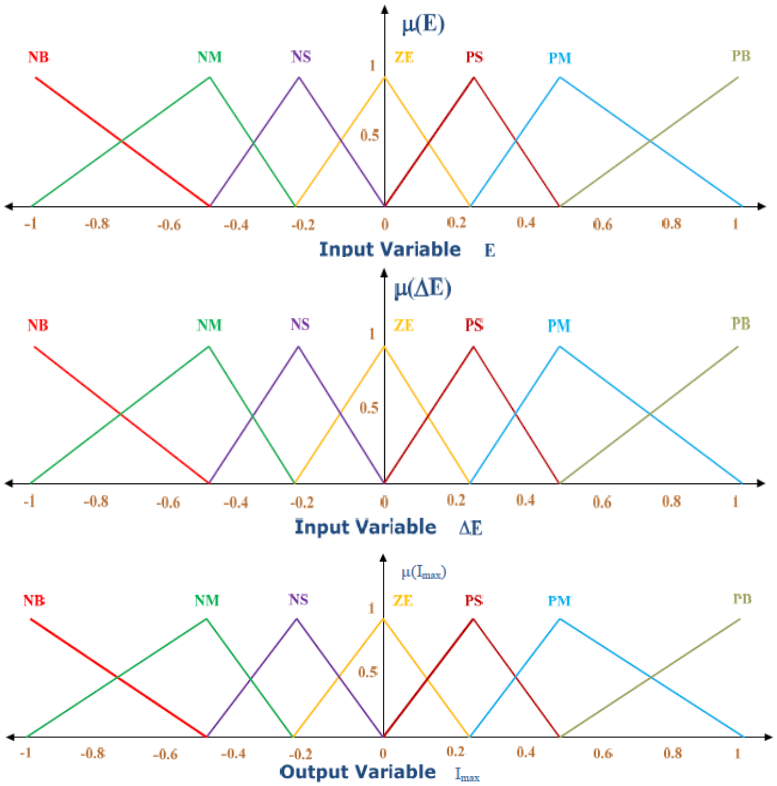

Fig. 10. Membership function for variable E, change in error CE and output.

6. Simulation and Experimental Results

The performance of the proposed PV-SAF simulated under three cases. Balanced/unbalanced source, balanced/unbalanced nonlinear load and UPS energy conservation mode.

Table 5 Design specifications for a three-phase PV-SAF simulated system

Description	Parameter	Value	Unit
AC Supply	Nominal Line Voltage	400	V
	Frequency	50	Hz
Load	Load Resistance	360	Ω
	Load Inductance	2	mH
Ripple Filter	Filter Inductance	40	mH
SAF	Filter Capacitance	25	μF
	Inductor	438	μH
	DC capacitor	2800	μF
	DC bus voltage	700	V
PV Module	No. of Solar cells	320	36
DC-DC converter	Nominal Voltage	48	V

Simulated results are presented for two cases. For these cases, the system frequency is maintained at 50 Hz and sample time is chosen to be 50 µsec. The input voltage of 400 V three-phase AC supply is given to load through three-phase programmable AC source. The switched-mode PWM VSI is made to operate at 180^0 conduction mode. Three-phase VSI is operated by six gate pulses generated from the PWM pulse generator. The PWM generator has pulse amplitude of 1V for all the six pulses. The system parameters considered for the analysis of the proposed PV-SAF are furnished in Table 5.

6.1. Case A: Balanced and unbalanced load

To analyze the performance of the proposed system under balanced load conditions, source voltage as well as source current is set as sinusoidal but not in phase. The SAF is required to compensate the reactive power only. At t=0.1, the inverter is switched on. At this instant the inverter starts injecting the compensating current so as to compensate the phase difference between the source voltage and current. The supply current is the sum of load current and injected SAF output current. During the initial period, there is no load deviation in the load. Hence, the programmable three-phase AC voltage source feeds the total active power of 2000 W to the load. Figure 11 shows the waveforms of load current (a), grid current (b), SAF compensating current (c) and neutral current (d). It's observed From Fig. 11(e) the real power generated from PV system is supply to the load required demand.

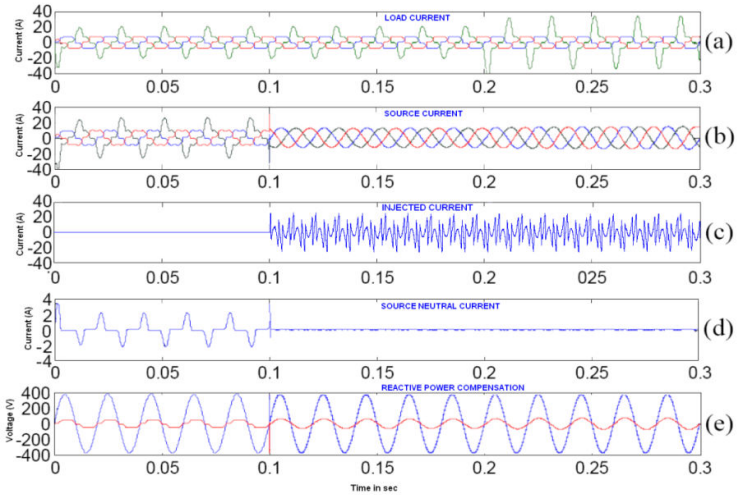

Fig. 11. Load current (a), source current (b), Injected current (c), neutral current (d) and reactive power compensation (e) under dynamic load changes.

During the unbalanced load condition, the transient load current changes occurs at times t=0.2s and 0.3s. It reduces the supplied active power of source from 2000 W to 1500 W as shown in Fig. 12. The resultant active power of the

load oscillates at 0.16 seconds and it stabilizes at 0.18 sec. During the period, the reactive power supplied by the source is reduced from 600 VAR to 210 VAR.

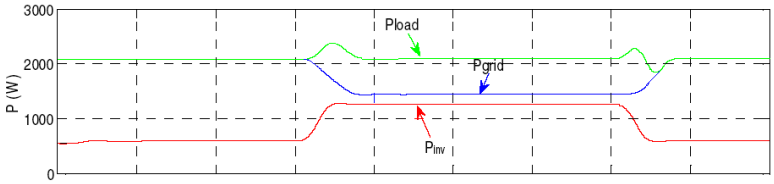

Fig. 12. Source, injected and load real power under dynamic load condition.

The SAF responds to the current transient and injects a reactive power of 500 VAR to restore the reactive power of the load. The results confirm the good dynamic performance of the SAF for a rapid change in the load current. The FFT of the grid current before and after compensation is carried out. The current THD is reduced from 21.54% to 1.53% as shown in Fig. 13.

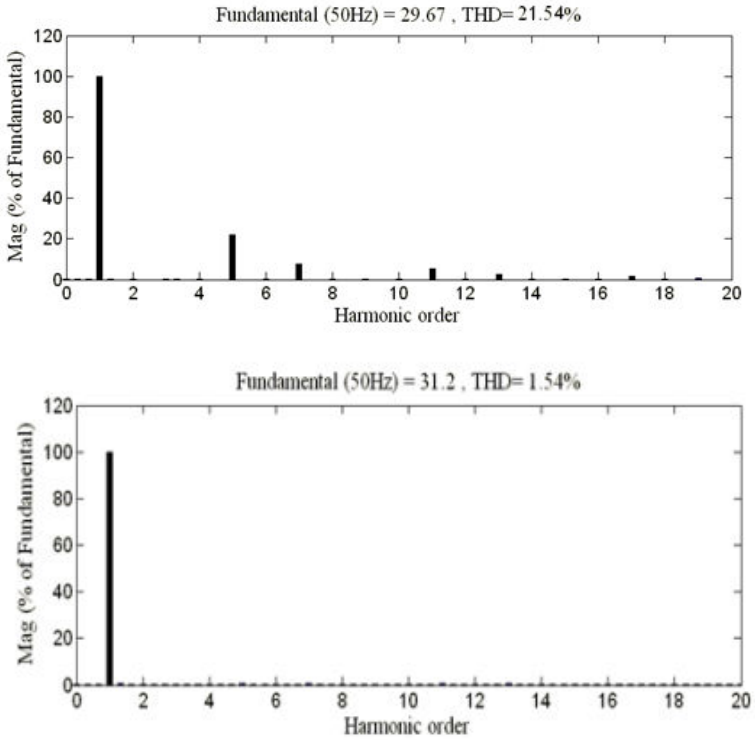

Fig. 13. Phase A current THD spectrum before and after compensation.

6.2. Case B: Energy conservation

The PV system is simulated with 10 number of 200W PV modules produce a total voltage and power of 60 V and 2000 W, respectively. Figure 14 shows the voltage, current and power at maximum power point, which is being tracked by fuzzy MPPT controller at different temperature and constant irradiation conditions. Figure 15 shows the response time of two MPPT controllers. At standard test condition, i.e., at irradiation of 2000 Watt/m^2 and temperature of 25^0 C the P&O MPPT controller is taking 0.1676 seconds to track the maximum power point whereas the fuzzy MPPT controller is taking only 0.0122 seconds to track the maximum power point. It concludes that the fuzzy based MPPT controller can reduce the maximum power tracking time by 88.18% as compared to conventional perturb and observe based MPPT controller.

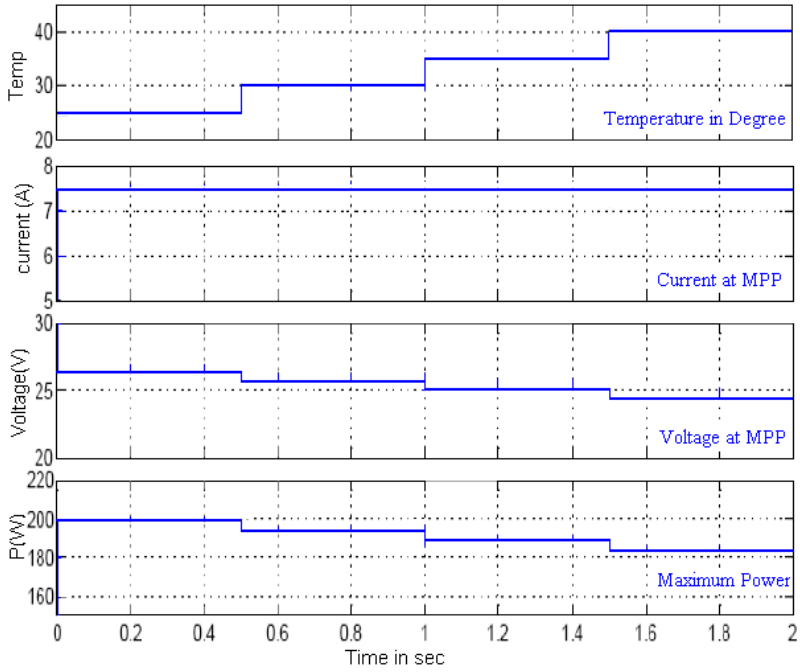

Fig. 14. Simulation result of maximum current, voltage and power with varying temperature and constant irradiation, i.e., at 1000 W/m^2 by fuzzy MPPT controller.

The DC-link voltage is decreasing during the compensation. The SAF supported DC-link capacitor consumes more power from the distribution system for the continuous compensation. Capacitor compensation is not enough for long transients. Taking these aspects into account, PV power generation system integrated with SAF is proposed in this work. In the conventional PI controller, the control parameters are fixed at the time of design. Hence, the conventional controller offers good performance only for the linear system. Capacitor

maximum overshoot and transient settling time as improved by fuzzy based control as shown in Fig. 15.

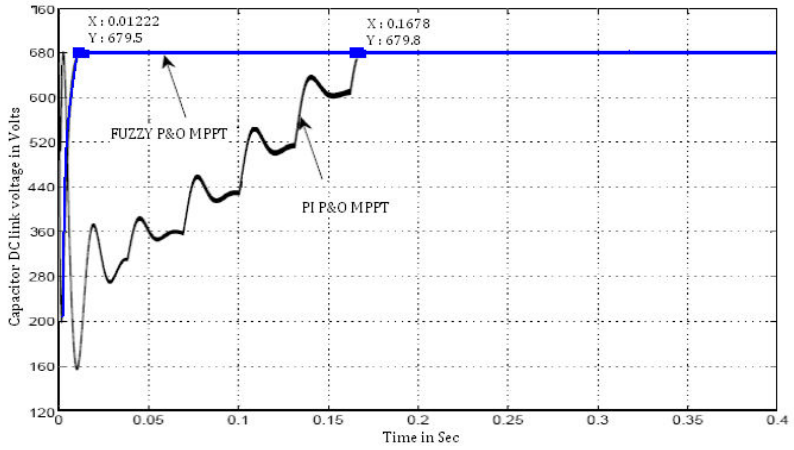

Fig. 15. Panel output by MPP Tracking P&O fuzzy logic controller method.

From Table 6 it's observed the fuzzy based ICosΦ controller is superior to the conventional PI control. When the power generation on the PV system is greater than the load demand, then the coordinating logic presented in the Table 2, connects the output of the PV system to manage the load demand. The RMS value of the supply voltage, injected voltage and load voltage of the SAF for energy conservation mode are shown in Fig. 16.

Table 6 PV-SAF response comparison.

Case under consideration	Maximum overshoot	Transient settling time	Source current THD %
conventional PI	96.5	0.053	7.26
Fuzzy	118.9	0.018	1.16

In this case, the SAF injects the nominal voltage of 400 V in parallel with the load. On examining the results, it is found that the proposed SAF is able to conserve the energy. This case provides an additional financial benefit to the users by reducing the power consumption from the utility grid. The active and reactive powers of the SAF in energy conservation mode are shown in Fig. 17. In this case, the SAF injects an active power of 2000 W and reactive power of 500 VAR to the load. The FFT analysis has been carried out for the balanced/unbalanced source and balanced/unbalanced load to determine the THD, which is illustrated in Table 7.

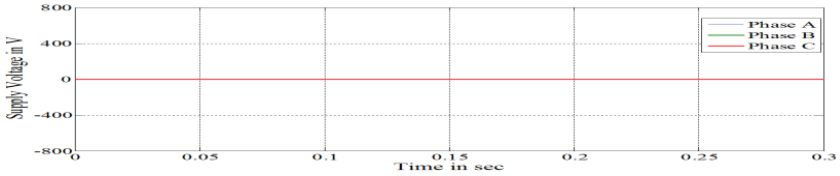

(a) Supply voltage

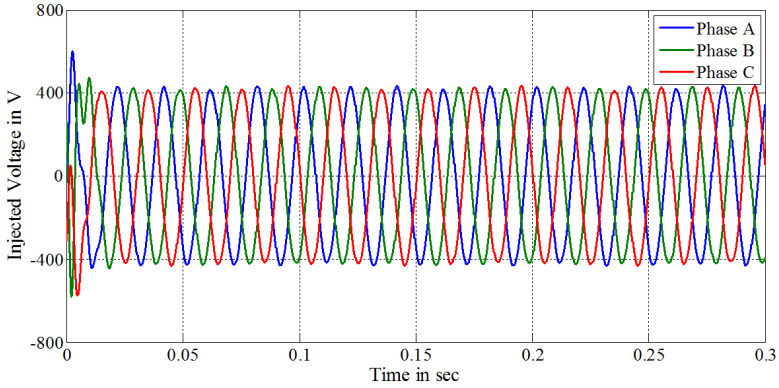

(b) Injected voltage

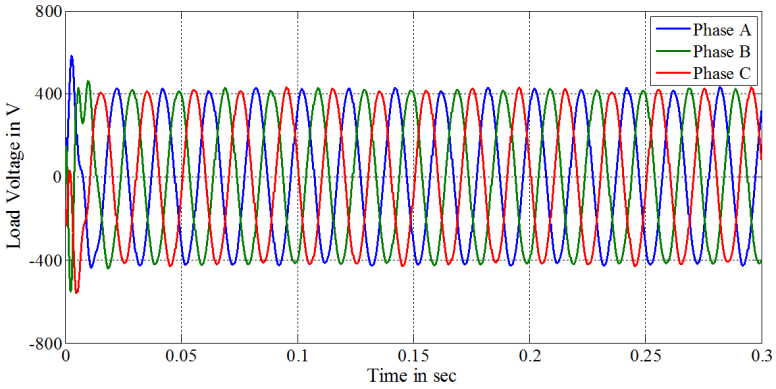

(c) Load voltage

Fig. 16. Supply injected and load voltage of the 3-phase PV-SAF.

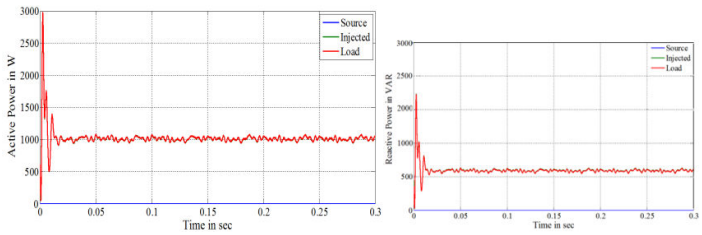

Fig. 17. Source injected and load active and reactive power of the PV-SAF.

Table 7. THD comparison without SAF compensation under different cases.

Source/load	Fundamental component of source current (p.u.)			THD in source current (%)		
Phases	A	B	C	A	B	C
Balanced source balanced nonlinear load	0.778	0.778	0.778	18.43	18.43	18.43
Unbalanced source balanced nonlinear load	0.516	0.759	0.328	19.23	20.90	25.40
Balanced source unbalanced Nonlinear load	0.676	0.741	0.627	21.54	22.40	20.90

6.3. Case C: Comparative study of experimental results

The experimental setup of PV-SAF as shown in Fig. 18. The result demonstrates the energy saving capability of the proposed SAF. The conventional SAFs presented in the literatures are only used for the compensation of current harmonics and reactive power. In the proposed SAF, additional function is added to fully utilize the energy generated by the PV power system.

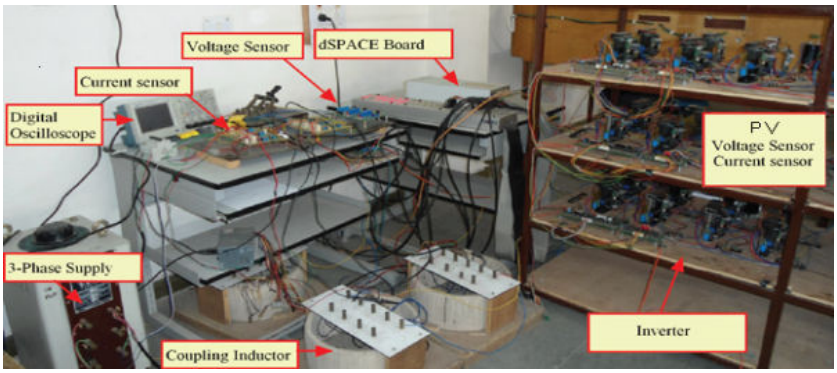

Fig. 18. Overall PV-SAF experimental setup.

It also helps to reduce the energy consumption of load from the three-phase utility distribution system. When the proposed coordinating logic, which is loaded in the FPGA controller detects the excessive or equal power generated by the PV system, the SAF enters into the energy conservation mode by disconnecting the three-phase supply voltage from the load and it configures that parallel to feed the real power generated on the PV system to load. The performance of PV-SAF demonstrates under unbalanced load in which, the current draw by load is integrated with harmonics. Figures 19(a) to (e) illustrates the performance of PV-SAF under Unbalanced sinusoidal voltage condition, THD for without SAF controller is 21.54%; THD for ICOSΦ method with PI Controller is 7.57%; THD

for ICOSΦ method with Fuzzy Controller is 3.6%. Figure 19(f) illustrates the capacitor voltage is maintained as constant magnitude.

Figure 19(c) illustrates the performance of PV-SAF injected current under un-balanced load condition, Even though the PI controller maintains the source current is inphase, but the current spike are increase the THD level as shown in the Table 8. It is observed that the proposed fuzzy controller based P&O MPPT controller tracked the maximum power generated by the PV array with 88.18 % of efficiency and also the proposed SAF ICOSΦ control maintains the THD below 5% as per IEEE519 standards.

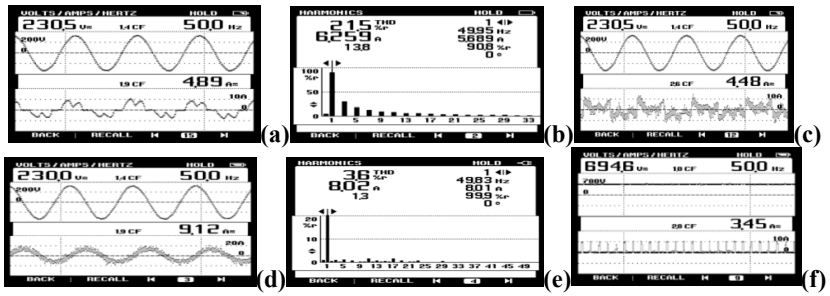

Fig. 19. SAF results under Unbalanced load condition.

Table 8. PV-SAF response comparison.

Method	THD in source current (%)		
	Balanced source &load	Unbalanced source & balanced load	balanced source &Unbalanced load
Without SAF	18.43	19.23	21.54
SAF with PI	7.26	7.35	7.57
PV-SAF ICOSΦ	3.42	3.58	3.6

7. Conclusion

This paper presents a novel application of utilizing a PV solar system as SAF for harmonic mitigation, reactive power compensation and neutral current compensation at the point of common coupling (PCC) at a small industry. A DC-DC converter with fuzzy controller based P&O MPPT algorithm is implemented to track the maximum power point of the PV array. When the operating point of view the system is changed, the parameters of the conventional controllers should be designed again, and some trials and prior information of the systems are needed to design the parameters. The fuzzy controller overcomes the drawbacks of the conventional controllers. A fast convergence with small oscillation at the maximum power point can be achieved by this method. This novel PV-SAF can reduce the energy consumption from the three phase utility grid, when the PV system generates excessive power or equal power to the load demand. Further, it reduces the energy consumption tariff and avoids the use of stabilizer for the

individual equipment at a residence, small industry, etc. The simulation and experimental results shows that the PV-SAF performance is satisfactory in mitigating the current harmonics for the operation over 24×7 hours and reduces the THD level as per the IEEE519 standard.

References

1. Vijayakumar, G.; and Anita, R. (2013). Renewable energy interfaced SAF using PI controller based ant colony and swarm optimization algorithms. *Australian Journal of Basic and Applied Sciences*, 7(8), 110-119.
2. El-Habrouk, M.; and Darwish, M.K. (2000). Active power filters: a review. *IEEE Proceedings on Electric Power Applications*, 5(1), 403-413.
3. Akagi,H,; and Kanazawa,Y. (1984), Instantaneous Reactive Power Compensators Comprising Switching Devices without Energy Storage Components. *IEEE Transactions on Industry Applications*, 20(3), 625-630.
4. Salmeron, P.; and Herrera, R.S. (2006). Distorted and Unbalanced Systems Compensation within Instantaneous Reactive Power Framework. *IEEE Transactions on Power Delivery*, 2(3), 1655-1662.
5. Mohan, N.; and Undeland, T.M. (2006), Power *Electronics Converters: Applications and Design,* Third Edition, Jhon Wiley & Sons Asia Pvt. Ltd., Singapore, 172-178.
6. Bhuvaneswari G,; and Nair, M.G. (2008). Design, Simulation, and Analog Circuit Implementation of a Three-Phase Shunt Active Filter using the ICosΦ Algorithm. *IEEE Transactions on Power Delivery,* 23(1), 1222-1235.
7. Altas, H.; and Sharaf, A.M. (2007). A photovoltaic array simulation model for MATLAB simulink GUI environment. in proceeding ICCEP'07 Conference 2007. Trabzon, 341-345.
8. El-Tayyan, A.A.; (2011), PV system behavior based on datasheet, *Journal of Electron Devices*, 9(1), 335-341.
9. Bader, N.; and Alajmi. (2013), A Maximum Power Point Tracking Technique for Partially Shaded Photovoltaic Systems in Micro grids. *IEEE Transaction on Industrial Electronics*, 60(4), 1596-1606.
10. Elgendy, M.A.; and Zahawi, B. (2012). Assessment of perturb and observe MPPT algorithm implementation techniques for PV pumping applications. *IEEE Transaction on Sustainable Energy*, 3(1), 21-33.
11. Jain, S.K. (2002), Fuzzy Logic Controlled Shunt Active Power Filter for Power Quality Improvement. *IEEE Proceedings Electric Power Applications*, 149(5), 317-328.
12. Kirawanich, P.; and Connell, R.M. (2004). Fuzzy Logic Control of an Active Power Line Conditioner. *IEEE Transactions on Power Electronics*, 19(6), 1574-1585.